



Calhoun: The NPS Institutional Archive

Theses and Dissertations

Thesis Collection

1967-06

The effect of surface waves on acoustic transmission in shallow water.

Halpin, Hugh

Brown University

<http://hdl.handle.net/10945/12066>



Calhoun is a project of the Dudley Knox Library at NPS, furthering the precepts and goals of open government and government transparency. All information contained herein has been approved for release by the NPS Public Affairs Officer.

Dudley Knox Library / Naval Postgraduate School
411 Dyer Road / 1 University Circle
Monterey, California USA 93943

<http://www.nps.edu/library>

NPS ARCHIVE
1967
HALPIN, H.

THE EFFECT OF SURFACE WAVES ON
ACOUSTIC TRANSMISSION IN SHALLOW WATER

HUGH HALPIN

THE EFFECT OF SURFACE WAVES
ON ACOUSTIC TRANSMISSION IN SHALLOW WATER

by

Hugh Halpin
"

Sc.B., Providence College, 1959

Thesis

submitted in partial fulfillment of the requirements for the
Degree of Master of Science in the Department of
Physics at Brown University

June, 1967

NPS ARCHIVE

1967

HALPIN, H

~~THESIS~~
~~H 1624~~

This thesis by Hugh Halpin
is accepted in its present form by the Department of
Physics as satisfying the
thesis requirement for the degree of Master of Science

Approved by the Graduate Council

Date:

TABLE OF CONTENTS

	Page
Acknowledgments	iv
SECTION I -- Outline of Problem	1
SECTION II -- Development of the Mathematical Model	6
SECTION III -- Evaluation of the Proposed Model	20
SECTION IV -- Discussion of Results and Limitations of Model	30

ACKNOWLEDGMENTS

It is a pleasure to express my sincere gratitude and deep appreciation to Professor Peter J. Westervelt, and to Professor Arthur O. Williams, Jr., for their guidance and encouragement throughout the course of this work.

SECTION I -- Outline of Problem

Several years ago J. A. Scrimger reported on measurements of the "Signal Amplitude and Phase Fluctuations Induced by Surface Waves in Ducted Sound Propagation."¹ This thesis is the result of attempts to develop a simple mathematical model capable of reproducing some of the results found by Scrimger.

The Esquimalt lagoon, located in British Columbia, Canada, was utilized in obtaining the experimental data. Embracing an area of approximately $1/4$ square mile, the lagoon has a tidal variation of two feet -- about a mean depth of 9 ft in summer, and the same variation -- about an 11 ft mean depth in winter. The water bottom consists of a clay sediment underlain by rock with sound velocities of 8300 and 17,500 ft/sec, respectively. The depth of the clay sediment varies throughout the lagoon but was determined to be 300 feet directly beneath the transmitter and 100 feet beneath the receiver. The hydrophones employed in the experiment were bottom-mounted on large tripods which extended several feet above the water's surface. The hydrophones were essentially omnidirectional, and located 300 feet apart throughout the tests. Surface-wave height was measured by recorders positioned on top of the tripods, the recorders consisting of styrofoam floats mechanically coupled to a potentiometer. The vertical movement of the floats, induced by surface waves, produced proportional output voltages which could be readily measured. Temperature gradients were obtained from a vertical set of five thermistors located midway between source and receiver.

In general it was found that perturbations in the form of surface water waves produced fluctuations in the received signal. These fluctuations were

¹J. A. Scrimger, J. Acoust. Soc. Am. 33, 239 (1961).

periodic and depended strongly on the amplitude and shape of the surface perturbation. In addition to the normal waves produced by wind and shifting tides, man-made waves were induced (the bow wave from a small power boat).

Frequencies generated at the transmitter ranged from 1 to 10 kc. The water waves produced by the wind attained amplitudes (crest to trough) approaching 3.5 in. in the upper limit. The fluctuations in the sound-pressure amplitude at the receiver due to the perturbation displayed several prominent features, viz. (1) the shape of the small-amplitude fluctuations matched closely those of the corresponding surface waves; (2) the fluctuations of larger amplitude exhibited, in addition, harmonics of the frequencies present in the surface waves; (3) the average values of both phase and amplitude fluctuations increased with the transmitted acoustic frequency.

Figure 1, drawn from Ref. 1, is a plot of average per cent fluctuation in signal amplitude vs. wave amplitude. For the lower frequencies (1-4 kc) the signal fluctuation increases with increasing wave amplitude, nearly linearly. In general, the slope of each curve becomes increasingly steeper as the acoustic frequency increases, and the linear relationship that held for increasing wave amplitudes at the lower frequencies is no longer applicable. The results at 5.9 kc, which appear to be inconsistent with the other data, were assumed in Ref. 1 to be attributable to variations in water depth caused by tides.

It was further noted in conjunction with Fig. 1 that fluctuations in excess of 30% were seldom observed, regardless of acoustic frequency.

In addition, as surface-wave height and frequency were increased, a point was reached above which the fluctuation spectrum recorded at the receiver was considerably broader than the surface wave spectrum and showed well defined second and higher harmonics not present in the surface wave. In both cases

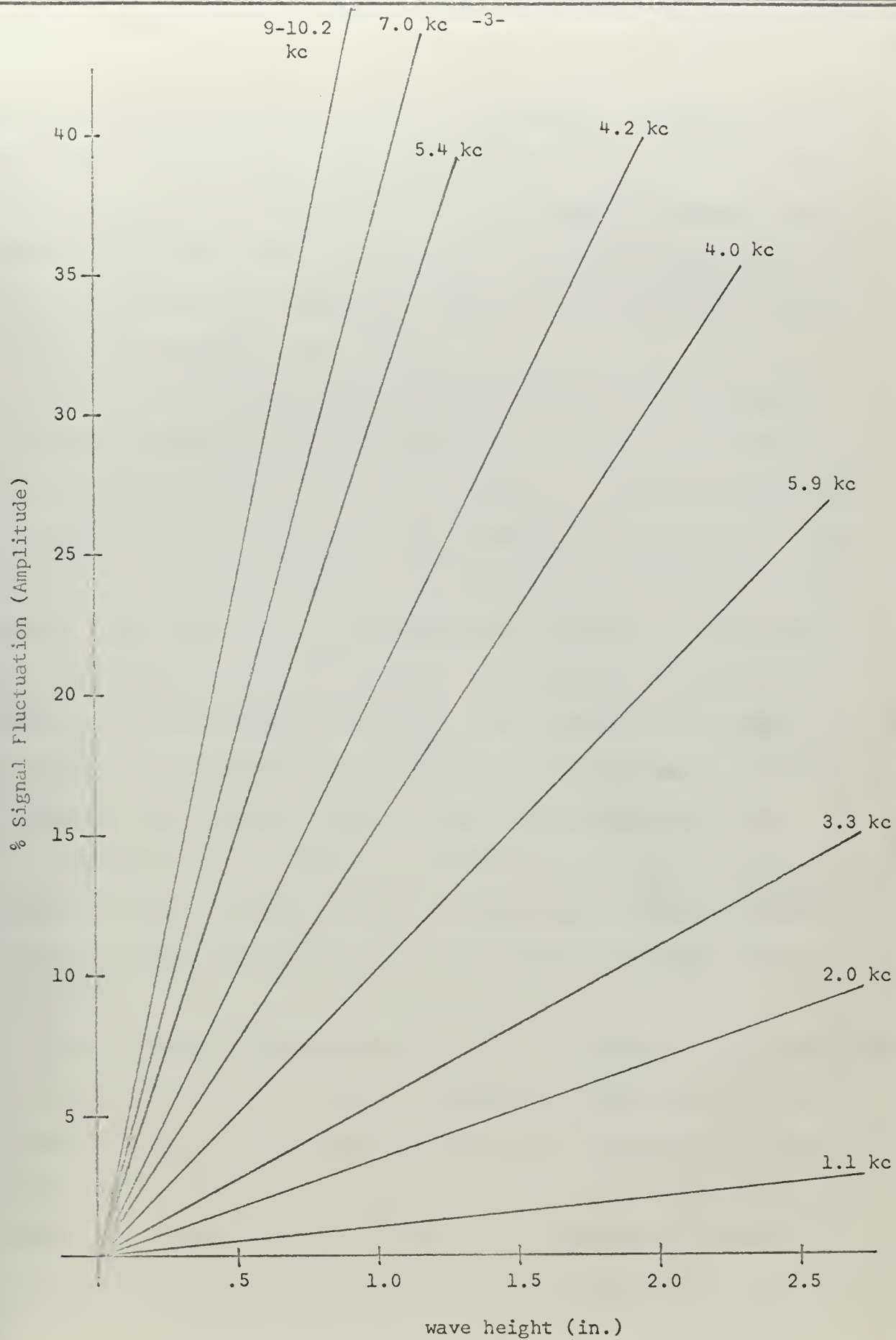


Fig. 1

Scrimger's measurements indicated that the significant parameter on which the fluctuations depend is the ratio of surface-wave height A to acoustical wavelength λ (λ/A). The value $\lambda/A = 18$ was found to provide a convenient dividing line between those fluctuation spectra containing appreciable second- and higher-order harmonic components ($\lambda/A < 18$) and those spectra containing only the first harmonic ($\lambda/A > 18$).

In an attempt to investigate the variation in the received signal amplitude as a function of surface perturbation position, wave packets were produced and the signal fluctuations were examined as the wave disturbance was propagated from the receiver toward the transmitter or, alternately, in the opposite direction. In practice the wave packets were created utilizing the bow wave from a small boat on an otherwise calm surface. In order to distinguish the bow wave from motor noise and waves produced at the stern of the vessel, the boat was pointed toward either the transmitter or receiver so as to avoid cutting the imaginary line connecting the two instruments, and the motor was stopped several seconds before the wave train reached the tripod.

The experiment was carried out initially using a single transmitted c.w. frequency. Later, in order to provide reliable results on the effect of changes in acoustic frequency, two c.w. sound signals were transmitted simultaneously.

Wave trains were propagated from receiver to transmitter and subsequently from transmitter to receiver for five frequencies ranging from 0.7 to 2.0 kc. The spectra recorded at the receiver indicated that fluctuations occurred only when the wave packet was in the immediate vicinity of either the source or receiver. As higher acoustic frequencies (up to 10 kc) were introduced, fluctuations in the received signal appeared when the surface wave was located at

greater distances from the source and receiver, but the maximum disturbances continued to occur when the perturbation was directly over source or receiver. A frequency was eventually reached (approximately 10 kc) which produced fluctuations at the receiver independent of the position of the wave packet. In all cases, the presence of harmonics in the signal fluctuations depended on λ/A as mentioned previously.

A summary of the conclusions drawn from Scrimger's paper follows:

1) The average fluctuation in received signal intensity increases with increasing frequency as well as the increasing wave height, up to a maximum fluctuation value of about 30%.

2) For large values of λ/A (i.e. acoustic wavelength to wave height), the shape of the fluctuating acoustic signal closely resembles the surface-wave shape, whereas small values of λ/A go with received fluctuations that are broader and that contain more harmonics than the surface wave. A convenient dividing line for λ/A separating the two cases was found to be approximately 18.

3) Propagating a wave packet over an otherwise calm surface, between source and receiver, showed fluctuations in low-frequency signals to occur mainly while the perturbation was near the source or receiver. However, with increasing acoustic frequency, the fluctuations were also observed for wave packet positions further removed from the source and receiver.

SECTION II -- Development of the Mathematical Model

As a first step in providing a theoretical explanation of Scrimger's results, the omnidirectional cw transmitter used as a sound source throughout the actual experiment can be replaced by a simple point source located a distance h below the water's surface. In an unbounded medium, this source spreads energy uniformly over a complete spherical surface at each radius " r " from the origin. The acoustic pressure P is given by the expression²

$$P = [i\rho_0 ckQ_0/(4\pi r)]e^{i(\omega t - kr)} \quad (2.1)$$

where

c = sound speed in the water

ν = frequency = $ck/2\pi$

ω = acoustic angular frequency = $2\pi\nu$

k = wave number = ω/c

ρ_0 = equilibrium density of water

r = distance from source to desired point in the sound field

Q_0 = strength of the simple source.

In addition, the problems encountered in dealing with the air-water interface can be simplified by considering the acoustic field as an interference effect between two sources: the original source, given by Eq. (2.1), located a distance h below the reflecting surface, and an image source of equal strength reflected in the air-water interface and located a distance h above the surface. The acoustic pressure for the image source is given by

²L. E. Kinsler, A. R. Frey, "Fundamentals of Acoustics," (John Wiley & Sons, Inc., New York, 1962, 2nd ed).

$$P = [-i\rho_0 v Q_0 / (2r)] e^{i(\omega t - kr)} \quad (2.2)$$

where r is now the distance from image to receiver and the minus sign, which indicates a 180° phase shift at the surface, satisfies the boundary condition that the total pressure given by adding Eq. (2.1) and (2.2), must vanish at the surface.

Combining Eq. (2.1) and (2.2), and recognizing that reflections from the bottom have been completely ignored, we have a dipole expression for the pressure amplitude at any point in the sound field (see Fig. 2);

$$P_D = [i\rho_0 v Q_0 / 2] [(e^{-ikr_1})/r_1 - (e^{-ikr_2})/r_2], \quad (2.3)$$

where r_1 = distance from point source to field point.

r_2 = distance from image source to field point.

It can readily be shown for spherical waves that the radial pressure gradient $\partial p / \partial r$ is related to the radial particle acceleration by

$$-\partial p / \partial r = \rho_0 \partial^2 \xi / \partial t^2$$

where the symbol ξ represents radial particle displacement.

Orienting the coordinate system as indicated in Fig. 2 with the origin located at the point 0, and considering only the y-component of particle motion (i.e., perpendicular to the air-water interface), we obtain the particular case

$$-\partial p / \partial y = \rho_0 \partial^2 \xi / \partial t^2 = \rho_0 a_y \quad (2.4)$$

where a_y is the particle acceleration in the y direction.

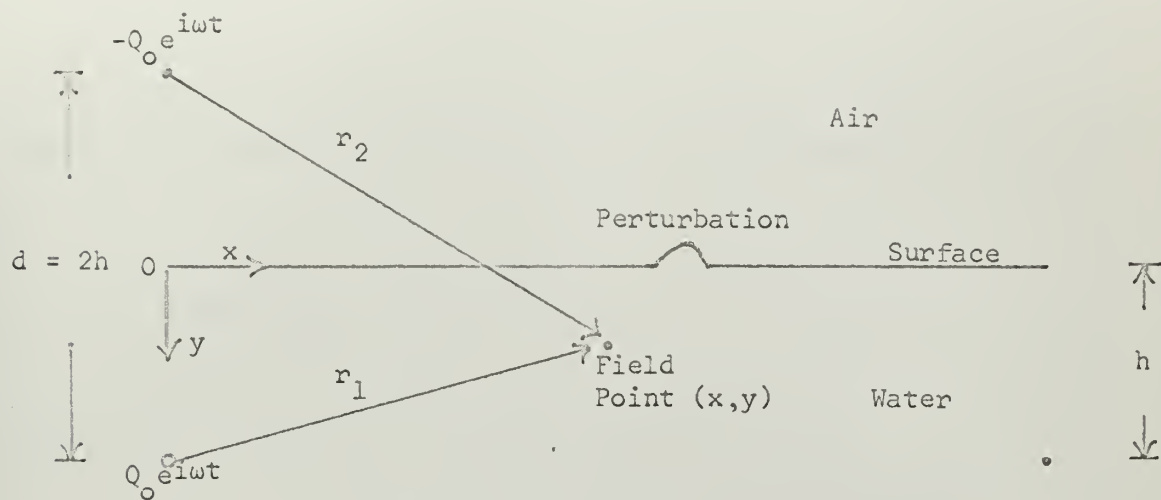


Figure 2

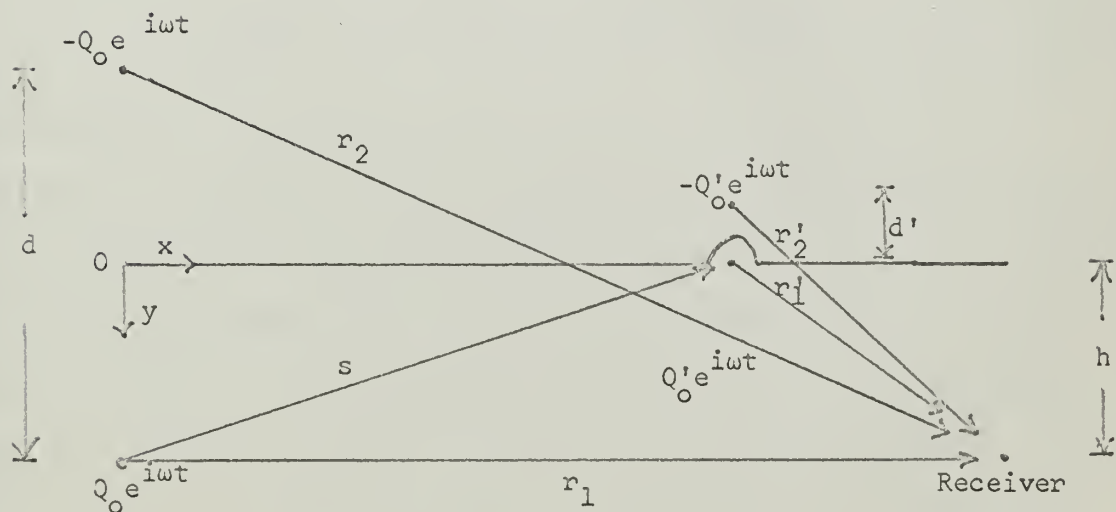


Figure 3

It is evident from Fig. 2 that r_1 and r_2 can be expressed as follows, in terms of x , y , and h :

$$r_{1,2} = [x^2 + (h \mp y)^2]^{1/2} \quad (2.5)$$

Substituting these expressions in Eq. (2.3), and using Eq. (2.4), yields for a_y

$$a_y = \partial/\partial y \{ (ivQ_0/2) e^{i\omega t} [(e^{-ikr_1})/r_1 - (e^{-ikr_2})/r_2] \}; \quad (2.6)$$

$$a_y = (-ivQ_0/2) e^{i\omega t} \{ [ik(h-y) e^{-ikr_1}]/r_1^2 + [(h-y) e^{-ikr_1}]/r_1^3 + [ik(h+y) e^{-ikr_2}]/r_2^2 + [(h+y) e^{-ikr_2}]/r_2^3 \}. \quad (2.7)$$

Letting $y \rightarrow 0$, i.e., considering only those particles located at the air-water interface, we obtain from Eq. (2.7)

$$a_{y0} = vhQ_0 e^{i\omega t} [(ke^{-iks})/s^2 - (ie^{-iks})/s^3], \quad (2.8)$$

where $s = [x^2 + h^2]^{1/2}$, the value of r_1 and r_2 when $y = 0$.

Thus far, the surface has been considered to be plane and free of waves. As a first approximation to the surface-wave perturbation, let us use a single symmetric pulse moving along the x axis and instantaneously located at x , as illustrated in Fig. 2. It is physically obvious that such a distortion in the reflecting interface will alter the acoustic field at the receiver. It is also obvious that this new effect vanishes as the height of the surface-wave pulse goes to zero, and, since the horizontal dimensions of the pulse are assumed to be very small compared with the distance from source to receiver, a plausible approach is to regard the disturbance in the acoustic field as coming

from a dipole, with a vertical axis, located at the pulse. The main task is to determine the strength of this dipole.

Letting P_D' represent the incremental acoustic pressure caused at (x,y) by the surface-wave -- which is assumed to act as if it were a dipole -- we can write

$$P_D' = [(ip_o v Q_o')/2] e^{i\omega t} [(e^{-ikr_1'})/r_1' - (e^{-ikr_2'})/r_2'] \quad (2.9)$$

where the perturbation-dipole strength Q' depends, in a manner to be determined, on the source-dipole strength Q , and the source separation d' for the perturbation dipole is proportional to the wave height (d' enters into r_1' and r_2' just as $d = 2h$ did in r_1 and r_2). Henceforth P_D , as given by Eq. (2.3), will be referred to as the "source dipole," and P_D' , as given by Eq. (2.9), will be referred to as the "perturbation dipole."

Figure 3 shows the distances needed to specify the pressure amplitude occurring at the receiver for an arbitrary position of the perturbation dipole.

If one calls the mass of the surface-wave pulse m , the vertical force F_y exerted by the field of the source dipole is given by

$$F_y = mvhQ_o e^{i\omega t} [(ke^{-iks})/s^2 - (ie^{-iks})/s^3] = F_o e^{i\omega t}, \quad (2.10)$$

where a_{yo} is determined from Eq. (2.8).

In the preceding paragraphs we have succeeded in specifying the particle acceleration due to the source dipole P_D , anywhere on the surface of the air-water interface. In addition, through knowledge of the surface-wave mass, the force exerted by the original acoustic field upon the perturbation is given by Eq. (2.10). We now attempt to express the perturbation-dipole strength Q' in terms of this force.

The fluid volume in the wave pulse is subject to the dynamics of moving compressible fluids and therefore certain conservation laws hold:

I. The Equation of Continuity --

$$\partial \rho / \partial t + \nabla \cdot (\rho \underline{y}) = 0, \quad (2.11)$$

where \underline{y} is particle velocity.

This equation expresses the fact that for a unit volume there is a balance between the change in density and the masses entering and leaving the system per unit time.

A source function can be inserted into the continuity equation to account for the rate at which mass is introduced. Thus Eq. (2.11) becomes

$$\partial \rho / \partial t + \nabla \cdot (\rho \underline{y}) = \rho_0 q, \quad (2.12)$$

where

ρ = instantaneous density

ρ_0 = equilibrium density

q = strength density.

Since the spatial variation of density is much less than the spatial variation of the particle velocity, Eq. (2.12) reduces to

$$\partial \rho / \partial t + \rho_0 \nabla \cdot \underline{y} = \rho_0 q. \quad (2.12a)$$

II. Conservation of Momentum --

$$\rho_0 (\partial \underline{y} / \partial t) + \rho_0 (\underline{y} \cdot \nabla \underline{y}) + \nabla p = \underline{f}. \quad (2.13)$$

Equation (2.13) is simply Euler's equation of motion for fluid flow, with p the pressure, and \underline{f} the external force exerted on the fluid. The mass of

fluid being considered is that in the surface-wave pulse, which is located essentially at $y = 0$. Equation (2.7) shows that for $y = 0$ the particle acceleration a_{y0} is independent of y . Therefore v_{y0} , which is merely the time integral of a_{y0} , is also independent of y . Hence v has at most only x - and z -components. But we are assuming that at the pressure-release surface the particle velocity v is v_y only -- i.e., particles move only normal to the surface. It follows that in the perturbation pulse $\underline{y} \cdot \nabla \underline{y}$ vanishes, and Eq. (2.13) reduces to

$$\rho_0 (\partial \underline{y} / \partial \tau) + \nabla p = \underline{f}. \quad (2.13a)$$

Taking $\partial / \partial t$ throughout Eq. (2.12a), operating with $(-\nabla \cdot)$ throughout Eq. (2.13a), and adding the results gives

$$\partial^2 p / \partial t^2 - \nabla^2 p = \rho_0 (\partial q / \partial t) - \nabla \cdot \underline{f}. \quad (2.14)$$

We assume that the fluid is homogeneous and nondissipative, so that any change $\Delta \rho$ in the density is proportional to an accompanying change Δp in the pressure:

$$\Delta \rho = \Delta p / c^2, \quad (2.15)$$

where c is the speed of sound in the fluid. It follows that $\partial^2 \rho / \partial t^2$ can be replaced by $c^{-2} \partial^2 p / \partial t^2$, and Eq. (2.14) becomes

$$c^{-2} (\partial^2 p / \partial t^2) - \nabla^2 p = \rho_0 (\partial q / \partial t) - \nabla \cdot \underline{f}. \quad (2.14a)$$

Since the single pulse representing the surface perturbation is assumed to be very small compared to the area of the calm surface, the external force

exerted on the wave by the source dipole can be approximated by a delta-function:

$$\underline{f} = \underline{F}\delta(\underline{r}-\underline{r}_0) = \underline{F}_0 e^{i\omega t} \delta(\underline{r}-\underline{r}_0), \quad (2.16)$$

where \underline{r} has components x, y, z , and the center of the wave pulse is at \underline{r}_0 .

The strength density q in Eq. (2.12a) can be written in the desired dipole form, as

$$q = Q\underline{d} \cdot \nabla [\delta(\underline{r}-\underline{r}_0)], \quad (2.17)$$

where Qd is the dipole strength of the perturbation dipole (Eq. (2.9)) and \underline{d} is the vector separation of the two point sources in this dipole. Then Eq. (2.14a) becomes

$$\begin{aligned} c^{-2}(\partial^2 p / \partial t^2) - \nabla^2 p &= \rho_0 (\partial Q / \partial t) \underline{d} \cdot \nabla [\delta(\underline{r}-\underline{r}_0)] - \nabla \cdot [\underline{F}\delta(\underline{r}-\underline{r}_0)] \\ &= \nabla \cdot [\rho_0 (\partial Q / \partial t) \underline{d} \delta(\underline{r}-\underline{r}_0) - \underline{F}\delta(\underline{r}-\underline{r}_0)]. \end{aligned} \quad (2.18)$$

The last step is allowed because $(\nabla \cdot)$ does not operate on the constant ρ_0 , nor upon Q and d , which are assumed to be independent of x, y, z (i.e., the perturbation wave does not change shape as it travels, and therefore the associated perturbation dipole does not change shape, either). Also, $(\nabla \cdot)$ and $\partial/\partial t$ can be assumed to commute.

Equation (2.18) has been developed for the general case in which both a generating source q and an external force \underline{f} are present. In the true physical situation of this problem, there is no source putting fluid into the wave, but there is an external force \underline{f} produced by the original source dipole. Then the right-hand side of Eq. (2.18) reduces to

$$- \nabla \cdot [\underline{F} \delta(\underline{r} - \underline{r}_0)]. \quad (2.19)$$

If, on the other hand, there had been a source but no external force, the right-hand side would have been

$$\nabla \cdot [\rho_0 (\partial Q / \partial t) \underline{d} \delta(\underline{r} - \underline{r}_0)]. \quad (2.20)$$

Therefore Eq. (2.18), which governs the acoustical behavior of the surface-wave pulse, would be unchanged if we postulate a nonphysical source whose effect in Eq. (2.18) is identical with that of the actual external force \underline{f} :

$$\nabla \cdot [\rho_0 (\partial Q / \partial t) \underline{d} \delta(\underline{r} - \underline{r}_0)] = - \nabla \cdot [\underline{F} \delta(\underline{r} - \underline{r}_0)],$$

or, after cancellations of the operators and of the common factor $\delta(\underline{r} - \underline{r}_0)$,

$$(\partial Q / \partial t) \underline{d} = \underline{F} / \rho_0. \quad (2.21)$$

Evidently \underline{d} , the vector separation in the nonphysical dipole, must be parallel to the external force \underline{F} .

In our particular case, \underline{f} and \underline{F} must be normal to the pressure-release interface between air and water. Hence \underline{F} and \underline{d} reduce to their own y-components. From Eq. (2.16), F equals $F_0 e^{i\omega t}$, and to be consistent with the notation in Eq. (2.9) we can write

$$Q = Q'_0 e^{i\omega t}. \quad (2.22)$$

From Eqs. (2.16), (2.21), and (2.22) it follows that

$$Q'_0 = F_0 / (i\rho_0 \omega d') \quad (2.23)$$

Obtaining F_0 from Eq. (2.10), we finally arrive at an expression for P'_D of Eq. (2.9):

$$P_D = \{mvhQ_0 e^{i\omega t}\} / 4\pi d' [(e^{-ikr_1^i})/r_1^i - (e^{-ikr_2^i})/r_2^i] [(ke^{-iks})/s^2 - (ie^{-iks})/s^3] \quad (2.24)$$

The acoustic pressure P at any point in the sound field is given by

$$P = P_D + P_D', \quad (2.25)$$

where the unperturbed (and major) part P_D comes from Eq. (2.3) and the small perturbation part from Eq. (2.24). The wave height appears implicitly in P_D' because the proportional quantity d' (Fig. 3) enters into r_2^i .

In an attempt to reproduce Fig. 1, using the model just developed, certain modifications are introduced in order to adapt the model to the physical situation.

In the actual experiment performed by Scrimger, the per cent signal fluctuations were obtained directly from magnetic tape and strip charts used to record the variations in pressure amplitude. Straight lines were drawn through the upper and lower average level of the peaks in the fluctuating signal to give the quantity ΔI for the over-all fluctuation. This was then related to the mean signal level I by the expression $\Delta I/2 \times 100/I$ to produce the per cent fluctuation. We shall hereafter omit "100," using the relative fluctuation $\Delta I/I$.

Although, as noted above, the original article expresses the per cent fluctuation in terms of pressure amplitude, it was found more convenient to consider this percentage as a function of signal intensity. For small values, $\Delta I/I \approx 2\Delta P/P$.

The pressure amplitude at the receiver due to the source dipole is given by Eq. (2.3) as

$$P_D = \frac{1}{2} i \rho_o v Q_o e^{i\omega t} [(e^{-ikr_1})/r_1 - (e^{-ikr_2})/r_2]. \quad (2.3)$$

Now

$$r_2 = [r_1^2 + (2h)^2]^{1/2} = r_1 (1 + 4h^2/r_1^2)^{1/2} \quad (2.26)$$

and since $(2h)^2 \ll r_1^2$ at the receiver, the binomial expansion can be applied to Eq. (2.26), giving

$$r_2 \approx r_1 (1 + 2h^2/r_1^2). \quad (2.27)$$

Define

$$r_{12} = \frac{1}{2}(r_1 + r_2) = r_1 + (h^2/r_1) = r_2 - (h^2/r_2).$$

Then in the denominator of Eq. (2.3), r_1 and r_2 may be replaced by $r_{12} \pm h^2/r_{12}$. In addition, the exponentials appearing in Eq. (2.3) can be written

$$e^{-ikr_{12}} [e^{ikh^2/r_{12}} - e^{-ikh^2/r_{12}}],$$

where r_1 has been replaced by r_{12} which is nearly equal to r_1 (even for $k \approx 10 \text{ ft}^{-1}$, $kh^2/r_1 \leq \pi$) and the small difference between r_1 and r_{12} is negligible.

Thus Eq. (2.3) reduces to

$$P_D = \frac{1}{2} i \rho_o v Q_o e^{i\omega t} [(e^{-ikr_{12}})/r_{12}] [e^{(ikh^2)/r_{12}} - e^{(-ikh^2)/r_{12}}] \quad (2.28)$$

since $r_{12} \gg h^2/r_1$.

However, $[e^{(ikh^2)/r_{12}} - e^{(-ikh^2)/r_{12}}]$ is $2i \sin(kh^2/r_{12})$, so that

Eq. (2.28) becomes

$$P_D \approx -\rho_0 v Q_0 e^{i\omega t} [(e^{-ikr_{12}})/r_{12}] \sin(kh^2/r_{12}). \quad (2.29)$$

The pressure amplitude seen at the receiver due to the perturbation dipole is given by Eq. (2.24) as

$$P'_D = [mh/(4\pi\rho_0 d')] (\rho_0 v Q_0 e^{i\omega t}) [(e^{-ikr'_1})/r'_1 - (e^{-ikr'_2})/r'_2] [(ke^{-iks})/s^2 - (ie^{-iks})/s^3]$$

Since s takes on values from 10 to 300 ft and since $k \geq 1$ for all frequencies under consideration, we can neglect the term $i \exp(-iks)/s^3$, relative to $\exp(-iks)/s^2$, and Eq. (2.24) reduces to

$$P'_D = [mh/(4\pi\rho_0 d')] (\rho_0 v Q_0 e^{i\omega t}) [(ke^{-iks})/s^2] [(e^{-ikr'_1})/r'_1 - (e^{-ikr'_2})/r'_2]. \quad (2.30)$$

Now $r'_1 = [(r_1 - x)^2 + h^2]^{1/2}$ and

$$r'_2 = [(r_1 - x)^2 + (h + d')^2]^{1/2} \approx [(r_1 - x)^2 + h^2 + 2hd' + d'^2]^{1/2}. \quad (2.31)$$

Further, since $d'^2 \ll 2hd'$, we have

$$r'_2 \approx [(r_1 - x)^2 + h^2]^{1/2} [1 + (2hd')/[(r_1 - x)^2 + h^2]]^{1/2}. \quad (2.32)$$

But the first bracket in Eq. (2.31) is simply r'_1 and since $2hd' \ll r_1'^2$ in the second bracket, the binomial theorem can be employed and Eq. (2.31) reduces to

$$r'_2 \approx r'_1 + hd'/r'_1. \quad (2.33)$$

It should be noted at this point that for minimum r_1' (i.e., wave perturbation directly over receiver), Eq. (2.33) yields $r_2 = h+d'$. Also, $d' \ll h$, and so $r_2' - r_1' = hd'/r_1'$ is always much less than r_1' or r_2' . This agrees with the experimental picture.

Define

$$r_{12}' = \frac{1}{2}(r_1' + r_2') = r_1' + hd'/(2r_1') = r_2' - hd'/(2r_2'). \quad (2.34)$$

As in the development leading to Eq. (2.29), replace r_1' , r_2' in the denominators by r_{12}' and in the exponentials by $r_{12}' - hd'/2r_1'$ and $r_{12}' + hd'/2r_2'$ respectively. Carrying out the same procedures used to obtain Eq. (2.29) on the remaining exponential factors, we find for P_D'

$$P_D' = [(imkh)/(2\pi\rho_0 d')] (\rho_0 v Q_0 e^{i\omega t}) \{ [e^{-ik(r_{12}' + s)}] / r_{12}' s^2 \} \sin(khd'/2r_{12}'). \quad (2.35)$$

In both Eq. (2.27) and Eq. (2.33), the fact that the second term is much smaller than the first is not sufficient reason to employ the binomial expansion since all r 's are multiplied by k to form the exponents $e^{-ik\dots}$. The important test is that the next term in the binomial expansion — omitted here — upon multiplication by k yields a quantity much less than $\pi/2$. This condition is easily satisfied in each case.

Defining the intensity $I = CP^*P$, where $*$ indicates "complex conjugate," C is a dimensional constant of the same value for P_D and P_D' , and

$$P = \text{total pressure amplitude} = P_D + P_D',$$

we obtain the fluctuation intensity

$$\Delta I/I = (P_D P_D'^* + P_D^* P_D') / P_D P_D^* \quad (2.36)$$

having neglected the term $|P_D'|^2$.

In evaluating $\Delta I/I$, we note that the factor $\rho_0 v Q_0 e^{i\omega t}$ is common to both P_D (i.e., Eq. (2.29)) and P_D' (i.e., Eq. (2.35)) and so will cancel in Eq. (2.36). Applying Eqs. (2.29) and (2.35) to Eq. (2.36) and once again utilizing the fact that $e^{i\theta} - e^{-i\theta} = 2i \sin \theta$, we obtain

$$\frac{\Delta I}{I} = - \frac{V k h r_{12}}{d' \pi r_{12}' s^2} \left\{ \frac{\sin(k h d' / 2 r_{12}')}{\sin(k h^2 / r_{12})} \right\} \sin[k(r_{12}' + s - r_{12})] \quad (2.37)$$

where $V = m/\rho_0$ is the volume of the wave pulse.

SECTION III -- Evaluation of the Proposed Model

An examination of Eqs. (2.37) and (2.24) will help us to compare the behavior of these expressions with the results obtained by Scrimger.

The intensity fluctuation is given in Eq. (2.37) as

$$\Delta I/I = - \frac{V k h r_{12}}{\pi r_{12}'^2 s^2 d'} \left\{ \frac{\sin(k h d' / 2 r_{12}')}{\sin(k h^2 / r_{12})} \right\} \sin[k(r_{12}' + s - r_{12})]. \quad (2.37)$$

Equation (2.37) would be much simpler if each, or any, of the three trigonometric functions could be replaced by their respective arguments. We consider first $\sin(k h d' / 2 r_{12}')$. When the wave packet is directly over the receiver, r_{12}' takes on a minimum value which is practically equal to the water depth h , and the argument of the sine becomes $\frac{1}{2} k d'$. Figure 1, which is drawn from Scrimger's paper, shows that the maximum product of wave number k times wave height is 1.1. Since d' presumably approximates the wave height, this sine function can be replaced by its argument.* Thus Eq. (2.37) becomes

$$\Delta I/I = - \left(\frac{V k^2 h^2 r_{12}}{2 \pi r_{12}'^2 s^2} \right) \left\{ \frac{1}{\sin(k h^2 / r_{12})} \right\} \sin[k(r_{12}' + s - r_{12})] \quad (3.1)$$

and since d' makes only a negligible contribution to r_{12}' in the last sine term of Eq. (3.1), and appears nowhere else, it follows that, for $k d' \leq 1.1$,

$$\Delta I/I \propto V. \quad (3.2)$$

* Several points corresponding to 5.9 and 10.9 kc exceed this product. However, the points associated with each of these frequencies are inconsistent with the remainder of Fig. 1.

Consider next $\sin(kh^2/r_{12})$, in which h and r_{12} are constants such that $\sin(kh^2/r_{12})$ becomes approximately $\sin(k/3)$. To replace $\sin(k/3)$ with its argument requires that $k/3$ be no greater than 0.7, thus making $k \lesssim 2.1 \text{ ft}^{-1}$ (frequency 1.7 kc). For this value of $k/3$ the discrepancy between the sine and its argument is about 10%. When kh^2/r_{12} is substituted for the sine, Eq. (3.2) becomes

$$\Delta I/I \approx [(-V k r_{12}^2)/(2\pi r_{12}^2 s^2)] \sin[k(r_{12}' + s - r_{12})]. \quad (3.3)$$

Thus at low frequencies (i.e., less than 2kc), and still ignoring the last remaining sine term, $\Delta I/I$ varies with frequency in a linear manner. As $k/3$ rises to about $\pi/2$, $\sin(k/3)$ is nearly independent of frequency, and $\Delta I/I$ becomes proportional to ω^2 . When $k/3 \rightarrow \pi$, $\sin(k/3)$, as well as P_D , and $P_D P_D^*$, approach zero (see Fig. 4). The fact that $\Delta I/I$ approaches infinity when $\sin(k/3)$ approaches π can be attributed to the fact that the receiver is in the Lloyd-fringe region where small changes in frequency, or in h (tides, etc.), will produce large changes in the fluctuations measured at the receiver.

Still postponing an examination of $\sin k(r_{12}' + s - r_{12})$, consider the amplitude term $r_{12}'^2 s^2$ found in Eq. (3.3). In it, r_{12}' can safely be replaced by r_1' , and Fig. 3 shows that $s = (x^2 + h^2)^{1/2}$. Therefore we obtain

$$B \equiv r_{12}'^2 s^2 \approx [(r_1' - x)^2 + h^2](x^2 + h^2), \quad (3.4)$$

where the expression for r_1' is obtained from Eq. (2.34). Temporarily changing the coordinate system so that the origin is located midway between source and receiver (i.e., $x = r_1/2$) and letting $\eta = x - r_1/2$ alters Eq. (3.4) to the form

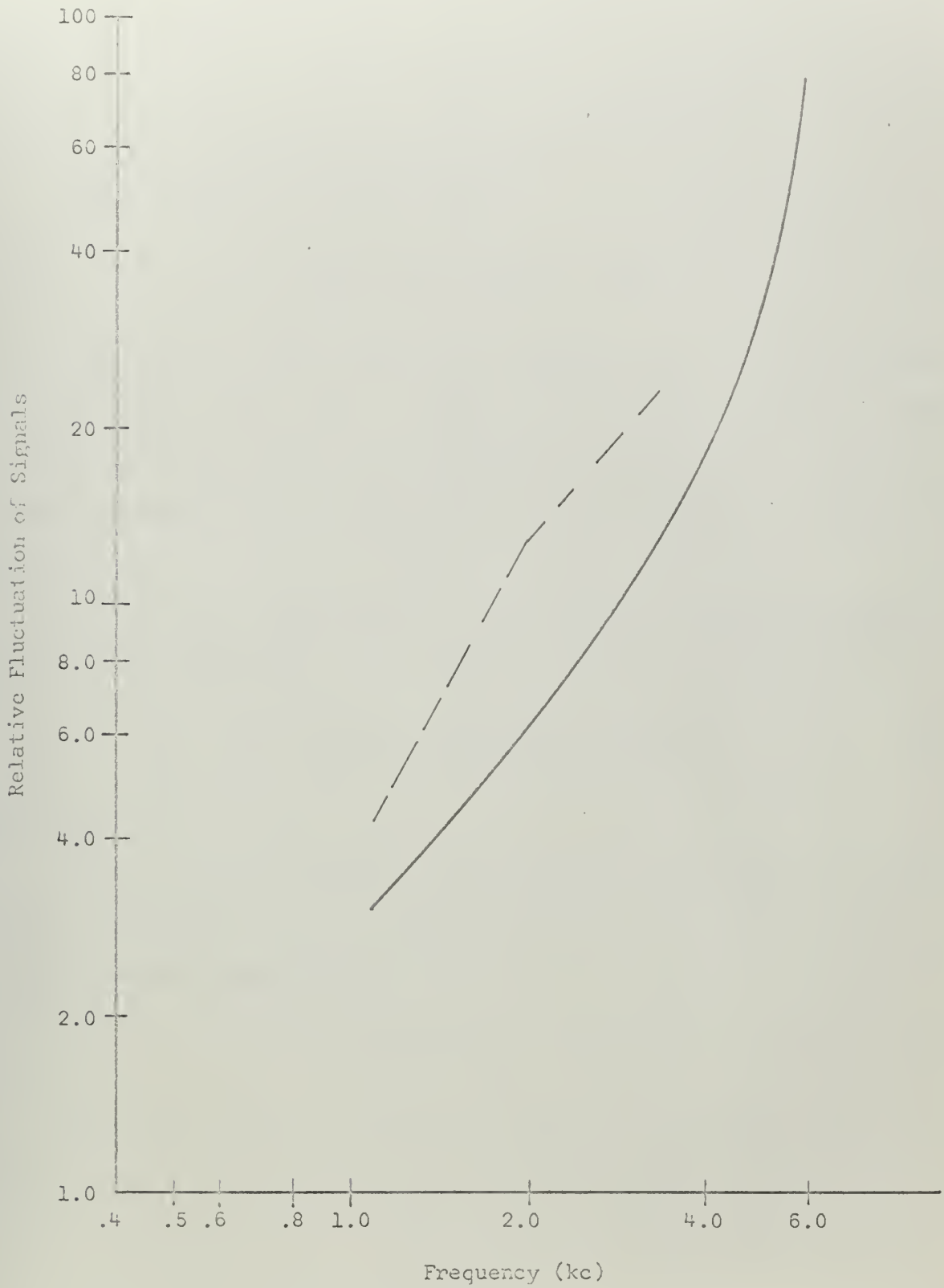


Fig. 4

$$B \approx [(\frac{1}{2} r_1 + \eta)^2 + h^2][(\frac{1}{2} r_1 - \eta)^2 + h^2]. \quad (3.5)$$

Equation (3.5) shows that $r_{12}^2 s^2$ is approximately symmetrical about the mid-range point (see Fig. 5), even for values of x to the left of the source and to the right of the receiver, as seen in Fig. 5.

Taking $dB/d\eta$ in Eq. (3.5) yields

$$dB/d\eta = 2\eta^3 - \frac{1}{2} r_1^2 + 2\eta h^2, \quad (3.6)$$

and setting $dB/d\eta = 0$ will disclose any maxima or minima in B (there are three such points since $dB/d\eta$ is cubic in η). Further, by taking $d^2B/d\eta^2$ and investigating the sign of the resultant expression, one can establish whether a maximum or minimum exists at any given η satisfying $dB/d\eta = 0$.

The results are

a) At $\eta = 0$ -- mid-range -- B has a maximum. Substituting the proper numerical values for r_1 , h and η into Eq. (3.5) produces

$$B = (\frac{1}{4} r_1^2 + h^2)^2 \approx r_1^4 / 16 \approx 5 \times 10^8 \text{ft}^4, \quad (3.7)$$

since $r_1^2 \gg h^2$.

b) At $\eta = \pm (\frac{1}{4} r_1^2 - h^2)^{1/2}$ -- i.e., nearly over the source or receiver but displaced slightly toward the center of the system -- there are minima, and Eq. (3.5) becomes approximately

$$B \approx h^2(r_1^2 + h^2) \approx 9 \times 10^6 \text{ft}^4. \quad (3.8)$$

Thus, still without considering $\sin[k(r_{12}' + s - r_{12})]$, Eqs. (3.3), (3.7), and (3.8) show that $\Delta I/I$ is about 50 times smaller when the wave pulse is at the mid-range position ($\eta = 0$) than when the wave pulse is approximately over the source or receiver (see Fig. 5).

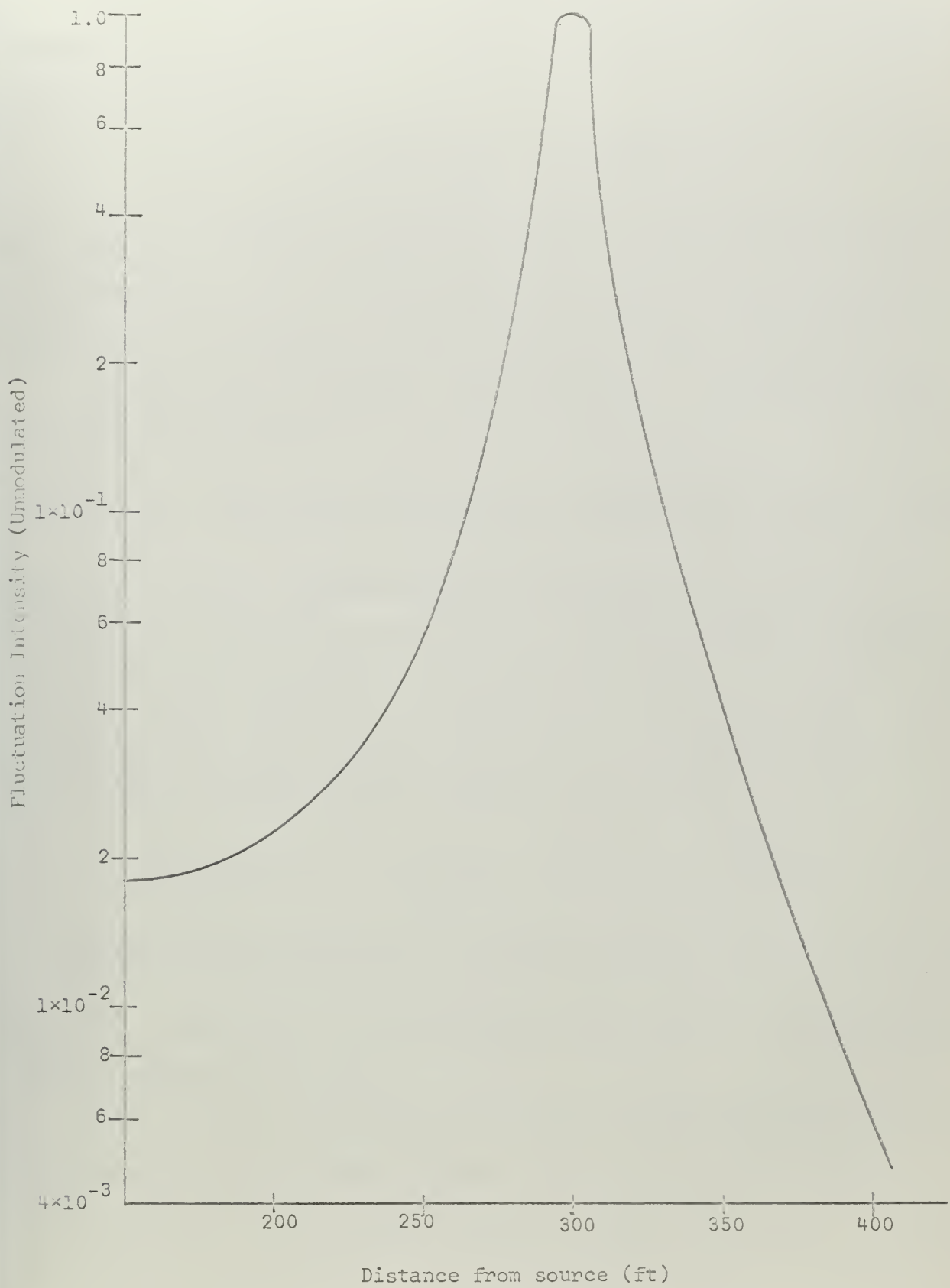


Fig. 5

Again investigating Eq. (3.4), assume that $x \ll r_1$, although not necessarily $\ll h$ (i.e., the wave pulse is in the vicinity of the transmitter). Equation (3.4) becomes

$$B \approx (x^2+h^2)(r_1^2+h^2) \approx r_1^2(x^2+h^2), \quad (3.9)$$

since $r_1^2 \gg h^2$. Thus the value of B is approximately symmetrical about the transmitter (at $x = 0$), and by a similar investigation over the receiver ($r_1 - x \ll r_1$), the same approximately symmetrical behavior is observed.

The last step is to analyze $\sin[k(r'_{12} + s - r_{12})]$. The argument of the sine term can be written as

$$r'_{12} + s - r_{12} = [(r_1 - x)^2 + h^2]^{1/2} + hd'/2r'_1 + (x^2 + h^2)^{1/2} - r_1 - h^2/r_1, \quad (3.10)$$

where r_{12} and r'_{12} have been defined in Section II and $s = (x^2 + h^2)^{1/2}$.

In order to investigate the behavior of Eq. (3.10) we consider three special cases: $|x| \ll r_1$; $|r_1 - x| = |\mu| \ll r_1$; $|x - \frac{1}{2}r_1| = |\eta| \ll r_1$. In Case 1, when x becomes small, r'_1 is nearly equal to r_1 , and the term $hd'/2r'_1$ in Eq. (3.10) can be written fairly accurately as $hd'/2r_1$:

$$(r_1^2 - 2r_1x + x^2 + h^2)^{1/2} + hd'/2r_1 + (x^2 + h^2)^{1/2} - r_1 - h^2/r_1 \quad (3.11)$$

$$= (r_1^2 + h^2)^{1/2} [1 - 2r_1x/(r_1^2 + h^2)]^{1/2} + hd'/2r_1 + (x^2 + h^2)^{1/2} - r_1 - h^2/r_1, \quad (3.12)$$

where x^2 appearing in the first brackets of Eq. (3.11) is considered negligible in comparison with $2r_1x$.

Using the binomial expansion on the term in brackets of Eq. (3.12), and multiplying by the first term, we have

$$(r_1^2 + h^2)^{1/2} - r_1x/(r_1^2 + h^2)^{1/2} + hd'/2r_1 + (x^2 + h^2)^{1/2} - r_1 - h^2/r_1. \quad (3.13)$$

Again using the binomial expansion on $r_1^2 + h^2$ in Eq. (3.13) and approximating $(r_1^2 + h^2)^{1/2} \approx r_1$ in the small terms that result, make Eq. (3.13) become

$$r_1 + h^2/2r_1 - x + hd'/(2r_1) + (x^2 + h^2)^{1/2} - r_1 - h/r_1 \quad (3.14)$$

$$= (x + h^2)^{1/2} - x - h^2/(2r_1) + hd'/(2r_1). \quad (3.14a)$$

Thus, for very small x (i.e., near the source), $\sin[k(r_{12}' + s - r_{12})]$ is given fairly accurately by

$$\sin\{k[(x^2 + h^2)^{1/2} - x - h^2/(2r_1) + hd'/(2r_1)]\}. \quad (3.15)$$

The other cases go similarly, after coordinate transformations from x to μ or to η are applied. Thus, Case 2, for small $\mu = x - r_1$, where $r_1' \approx h$, yields

$$\sin\{k[(\mu^2 + h^2)^{1/2} + \mu - h^2/(2r_1) + \frac{1}{2}d']\} \quad (3.16)$$

where it is noted that for large $x \approx r_1$, r_1' can no longer be replaced by r_1 but rather $r_1' \approx h$.

Case 3, for small $\eta = x - \frac{1}{2}r_1$ (i.e., mid-range), leads to the form

$$\sin\{k[h^2/r_1 + hd'/r_1 + hd'\eta/r_1^2]\}. \quad (3.17)$$

Comparison of (3.15) and (3.16) reveals that except for the terms in d' they behave symmetrically in their respective areas of influence if account is taken of the signs associated with x and μ : $x > 0$ means going from source toward receiver, whereas $\mu < 0$ means going from receiver toward source. Both terms in d' are small (d' is presumably a few inches at most).

Because of this similarity between (3.15) and (3.16), it suffices to examine (3.15) only.

When x goes to zero, (3.15) becomes

$$\sin\{k[h - (h/2r_1)(h-d')]\} \approx \sin(kh). \quad (3.18)$$

When $\eta \rightarrow 0$, (3.17) becomes

$$\sin\{k[h^2/r_1 + hd'/r_1 + hd'\eta/r_1^2]\} \approx \sin(kh^2/r_1). \quad (3.19)$$

Thus, even at the lowest frequency, 0.7 kc, considered here (corresponding to $k \approx 1$), the argument of this sine term changes from about 10 to 0.33 , i.e., from about 3π to about 0.1π , as x goes from 0 to $\frac{1}{2}r_1$. As x goes on from $\frac{1}{2}r_1$ to r_1 , the argument of the sine practically reverses this change. The change is proportional to k and therefore to frequency; e.g., at 5 kc the argument of the sine changes from about 20π down to 2π and back to about 20π , as x traverses the range from 0 to r_1 . Hence this sine term, the last factor in Eq. (2.37), can never be replaced by its argument. It modulates the overall change in $\Delta I/I$ produced by the variation of $r_{12}^2 s^2$ with x , making $\Delta I/I$ become alternately positive and negative (see Fig. 6).

In the region around mid-range, $(r_{12}^2 s^2)^{-1}$ is so small that it matters little what the sine term does, but near $x = 0$ and $x = r_1$ the effect of $\sin\{k[h - (h/2r_1)(h-d')]\}$ is important.

Since h and r_1 are fixed in this investigation, the exact value of $\sin\{k(r_{12}^2 + s - r_{12}^2)\}$ at $x = 0$ or r_1 depends mainly on k , though to a small extent on d' . The question arises, how rapidly does this term change near the source and receiver, where -- because of the small $r_{12}^2 s^2$ -- $\Delta I/I$ can be large?

To obtain an approximate answer, we neglect the small terms $-h^2/2r_1$ and $hd'/2r_1$, in Eq. (3.15). Regardless of the value of the sine at $x = 0$, it will be sure to have a zero when the argument changes by $\pm \pi$. Hence, to find the necessary change in x we write the argument of the sine for $x = 0$ and for x_0 and set the difference equal to $\pm \pi$:

$$2\pi h/\lambda - (2\pi/\lambda)[(x^2+h^2)^{1/2} - x] = \pm \pi, \quad (3.20)$$

with $k = 2\pi/\lambda$. Solving Eq. (3.20) for x yields

$$x \approx \frac{1}{2} \lambda (1 + \lambda/4h) \quad \text{or} \quad x \approx -\frac{1}{2} \lambda (1 - \lambda/4h), \quad (3.21)$$

for plus and minus π respectively.

Thus from Eq. (3.21) and Eq. (3.15), to the extent it can be trusted (i.e., only at small x), it is seen that when the wave pulse travels a distance λ , approximately but not exactly centered over the transmitter, $\sin\{k[(x^2+h^2)^{1/2} - x - h^2/2r_1 + hd'/2r_1]\}$ has at least two zeros (three, if (3.15) happens to be zero exactly at $x = 0$), and $\Delta I/I$ changes by a full cycle. A similar argument holds over the receiver, because (3.15) and (3.16) behave so nearly identically. In contrast, (3.17) shows that near mid-range the sine function scarcely changes with η , and so with x , but $\Delta I/I$ is small in that region, as we have noted.

$\Delta I/I$ as discussed depends -- except for its amplitude and part of its dependence on frequency -- mainly on P_D' (Eq. (2.24)). The same approximations used to obtain $\Delta I/I$ of Eq. (3.3) from Eq. (2.37) show

$$P_D' \approx (imkhvQ_0 e^{i\omega t}) / (4\pi d') [(khd'/r_{12}^2 s^2)] \{e^{-ik(r_{12}'+s)}\}. \quad (3.22)$$

It is obvious that the amplitude of P_D' depends on x via $r_{12}'^2 s^2$ just as did the amplitude of $\Delta I/I$. Hence, symmetry is present about $x = \frac{1}{2} r_1$, as well as for small $\pm \Delta x$ near $x = 0$, and $x = r_1$. Moreover, an examination of the conclusions drawn from (3.15) through (3.17) show that $k[r_{12}' + s - r_{12}]$ is nearly symmetric about the mid-range. Since r_{12} is a constant throughout the problem, $k(r_{12}' + s)$ must also possess this symmetry. Therefore we conclude that $e^{-ik[r_{12}' + s]}$, which represents the phase angle associated with the pressure amplitude of the perturbation dipole, is also approximately symmetrical about the mid-range.

Thus if a line is drawn perpendicular to the air-water interface and located midway between source and receiver (i.e., mid-range), the pressure amplitude detected at the receiver due to a surface wave located to the right of this line will produce nearly the same phase, at the receiver, as any wave in the corresponding position to the left of the reference line.

In short, P_D' has much the same properties as $\Delta I/I$. As a test of the low-frequency approximation introduced to obtain Eq. (3.3), some exact calculations of $|P_D'|$ have been made from Eq. (2.24) for several frequencies. The results are shown in Fig. 7 (pp 36, 37).

SECTION IV -- Discussion of Results and Limitations of Model

Before starting detailed comparisons of the present theory with Scrimger's measurements (Ref. 1), we point out that related but somewhat different quantities are used in the two cases. Most of Scrimger's conclusions present the time average of the magnitudes of measured fluctuations in the received acoustic pressure, converted to percentages of the magnitude of the average pressure itself. In this thesis it has been more convenient to deal with the value of $\Delta I/I$ produced when the perturbing wave pulse is at some specified position x . In Scrimger's case, many waves and trains of waves have passed by source and receiver for each plotted value of fluctuation. Hence we should imagine our wave pulse to pass over the whole range -- contributing strongly to fluctuations only when it is nearly over the source or the receiver -- and then evaluate an average of $\Delta I/I$ for values of x near 0 (or near r_1). The corresponding mathematical step is to replace $\sin[k(r_{12}^i + s - r_{12})]$ by the average of its magnitude, i.e., by $2/\pi$. There is also, of course, a factor of two between $\Delta I/I$ and $\Delta P/P$, and of 100 in converting to percentage, but these are constants and of no interest unless absolute magnitudes were to be compared.

The sine factor just mentioned is not always irrelevant. It would, for example, play an important part in discussing the frequency of individual fluctuations as a wave passes by. Therefore we prefer not to average over it except when this step is dictated by the nature of the experimental data.

Equation (2.37) proved reasonably successful in reproducing the experimental results determined from Fig. 1. An examination of the points making up the original graph in the Scrimger paper, upon which Fig. 1 is based, shows that for frequencies below 4 kc the fluctuations appear to have a linear dependence on wave height. For frequencies at and above 4 kc, this linear dependence becomes

questionable, the data points being quite widely scattered. As noted in Section III, $\Delta I/I$ is proportional to the volume V of the water-wave pulse. This volume is certainly dependent upon the wave height, since increasing the wave height certainly increases the volume, but it is necessary to see whether this dependence is linear or not.

The pulse wave treated in this thesis has, thus far, been only partly specified. It is quite small in horizontal dimensions -- e.g., much smaller than r_1 or h , and presumably not large compared with an acoustic wavelength; also, it has a height proportional to and presumably not much different from the related dipole separation d' . To make comparisons between theory and Scrimger's measurements, the wave pulse should be tailored in shape to resemble a piece of the sort of waves he used. Scrimger's Figs. 1-9 are associated with various trains of nearly parallel wave crests, with small heights, presumably extending a considerable distance. In any one test, the wave train had a fairly definite frequency ν_w , from about 1.0 to about 2.5 sec^{-1} in various cases. Therefore the waves had a fairly definite wavelength Λ which can be computed from Lamb.³

$$\Lambda \approx g/(2\pi\nu_w^2) \quad (4.1)$$

where g is the acceleration due to gravity. The amplitudes of the waves were always rather small compared with Λ , and therefore the waves were close to a sinusoidal shape in vertical section:⁴

$$u(x) \approx \frac{1}{2} \Lambda \cos(2\pi x/\Lambda). \quad (4.2)$$

³H. Lamb, "Hydrodynamics" (Dover Publications, New York, 1945, 6th ed.), p. 417.

⁴Ibid, p. 417.

The cross-sectional area of a part of such a wave is easily shown to be directly proportional to A (and to λ as well, but this is not relevant at present).

Hence we can define the shape of our wave pulse as follows: In the direction parallel to a wave crest, it will have a short constant length, not a function of x, λ, A , etc.; in the vertical plane at right angles to a wave crest, it will be shaped like part of a sinusoid. Then the volume V , as used in previous equations will be proportional to the wave height, or to Scrimger's A , or to d' . Accordingly, Eq. (3.3) shows that -- apart from the sine factor, which has been discussed separately -- the relative fluctuation in intensity is proportional to kA and so to A/λ . Thus the linear dependence of the fluctuations on wave height observed by Scrimger at any one frequency below 4 kc (and possibly for frequencies above this value) is confirmed by the results obtained in this work.

Figure 4 is a log-log plot of relative signal fluctuations vs frequency, from 0.7 to 6.5 kc, where the ordinates are proportional to the logarithms of $[\Delta I/I]/V$ from Eq. (3.1). The theoretical curve in Fig. 4 is linear in frequency near $\nu = 1$ kc, increases to a quadratic dependence in the vicinity of $\nu = 2.5$ kc, and finally approaches infinity as $\nu \rightarrow 7$ kc. This last phenomenon is attributable to the fact that for high frequencies the receiver is still in the Lloyd-fringe region, and near 7 kc P_D should theoretically go to zero, making $\Delta I/I$ approach infinity. In the neighborhood of 7 kc, small changes in frequency or in water depth will produce large changes in the fluctuations obtained at the receiver. The experimentally obtained curve of Scrimger is also plotted in Fig. 4, for frequencies from 1.1 to 3.3 kc. It shows a nearly quadratic dependence upon frequency as ν shifts from 1.1 toward 2.0 kc; as ν increases from 2.0 to 3.3 kc, this dependence becomes more nearly linear, the average slope between 1.1 and 3.3 kc showing a dependence midway between

linear and quadratic. Thus in the region between $\nu = 0.7$ and 4 kc the frequency dependence of $\Delta I/I$ predicted by our mathematical model is in fairly good agreement with Scrimger's experimental results. For frequencies higher than 4 kc this agreement breaks down; however, above 4 kc the reasoning used in Section III to replace $\sin(kh^2/r_{12})$ terms by its argument also loses its validity.

Figure 5 is a semi-log plot of $(r_{12}'^2 s^2)^{-1}$ vs distance from the source, to show the unmodulated symmetry present in Eq. (3.3). Figure 5 investigates $(r_{12}'^2 s^2)^{-1}$ from mid-range (i.e., 150 ft to the right of the source) to a point 100 ft to the right of the receiver (i.e., 400 ft right of the source). Calculations carried out for wave-pulse positions in an equivalent region about the source produce the same results.

Under the restriction of low frequencies that was applied to simplify Eq. (2.37), the form of $\Delta I/I$ as a function of x -- i.e., of the wave pulse's location -- is sketched in Fig. 6. The curves are restricted to values of x between 285 ft and 315 ft, to allow showing sufficient detail. Again, results computed for a similar region about the source produce identical results; the effect of Eq. (2.37) about the mid-range is negligible as noted earlier. The lighter lines (i.e., the envelope) represent $(r_{12}'^2 s^2)^{-1}$; modulation by the term $\sin k(r_{12}' + s - r_{12})$ produces the heavy lines.

Scrimger's data often employed regular trains of waves passing over the range, with frequencies ν_w from approximately 1.0 to 2.5 cps, as noted earlier. Investigation of Eq. (4.1) shows that Λ ranged approximately from 5 ft to 1 ft. It follows from this and from Fig. 6 that if $\Lambda \ll \lambda$ the modulation induced in $\Delta I/I$ will vary with Λ and therefore with the frequency of the water waves. If instead $\Lambda \gg \lambda$, the fluctuations shown in Fig. 6 should dominate; these will recur with a frequency given roughly by the speed of the water waves divided by the acoustic wavelength. Actually, neither condition is fully met, since

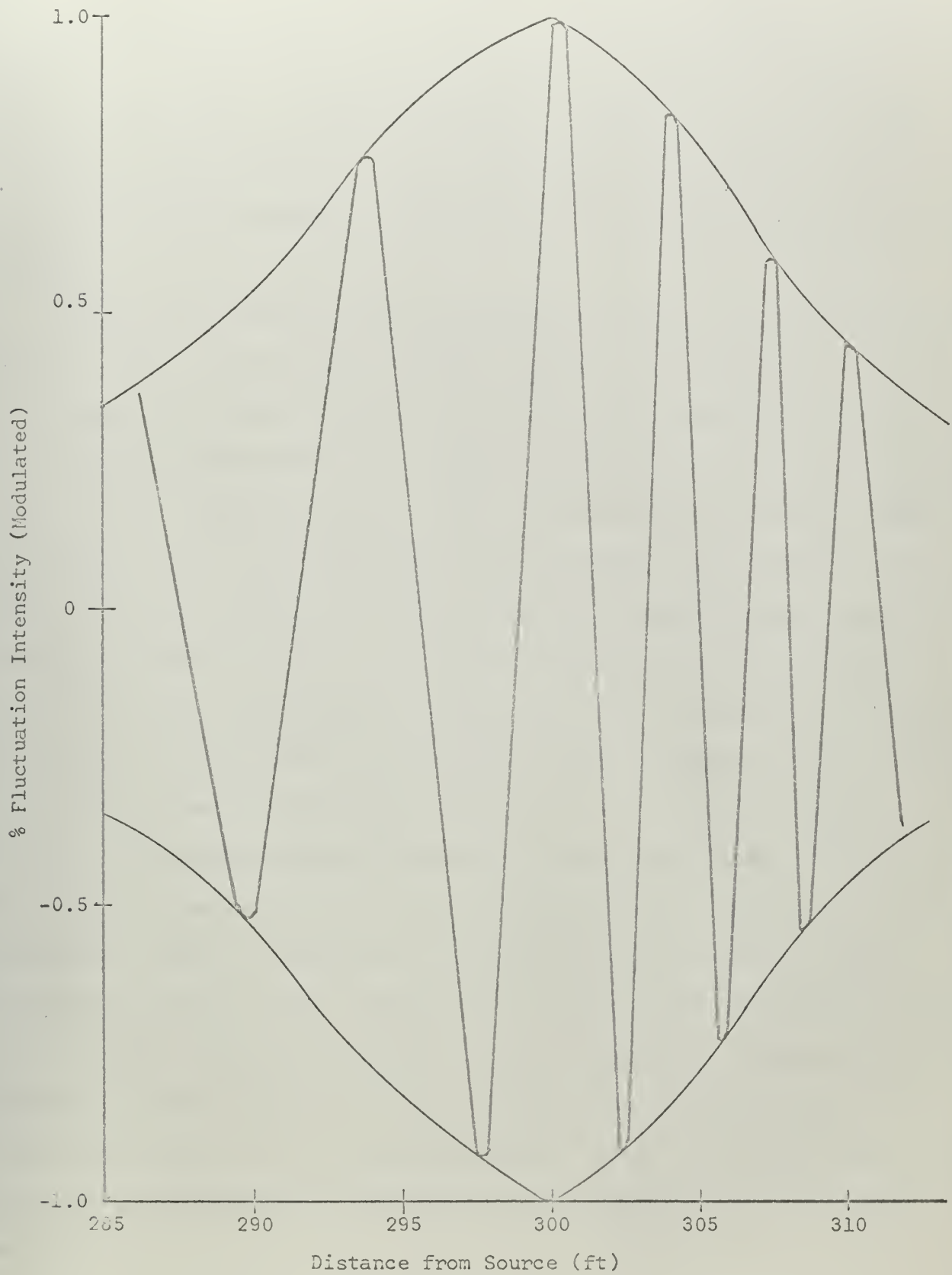


Fig. 6

λ varies from 1 to 5 ft for the frequencies under consideration, and one would expect $\Delta I/I$ to show a mixture of the two rates of variation. Finally, it is well to remember here than when considering a continuous wave train the total P'_D becomes a phase-dependent sum of several P'_D 's from individual waves located over both the source and receiver, thus further complicating the measured patterns.

Figure 7 is a semi-log plot, vs horizontal distance x of the wave pulse from the source, of the quantity $P'_D P'_D = |P'_D|^2$ as calculated from Eq. (2.24) before various approximations were introduced. In the calculations a value of 1.14 inches was chosen for d' , intermediate between the extremes of A given in Ref. 1. The absolute values of $|P|^2$ are unknown here, since they depend on both Q_0 and V ; but the correct relative heights are maintained in all cases. The Figure serves as a partial check on the approximations, introduced earlier, to obtain P'_D and $\Delta I/I$. The following points are noteworthy.

- (a) $|P'_D|^2$ behaves approximately the same whether the wave pulse is over source or receiver, but more nearly the same at low acoustic frequencies than at high.
- (b) $|P'_D|^2$ is more than 10^3 times as great for $x \approx 0$ or r_1 than for $x \approx \frac{1}{2} r_1$ (the approximations of Section III would predict about 50^2 or 2500).
- (c) $|P'_D|^2$ increases for all x with increasing acoustic frequency. (d) To some extent there is confirmation of Scrimger's observation that at higher frequencies fluctuations are observable even when the surface perturbations are near mid-range. The ratio of maximum to minimum in Fig. 7 is practically independent of acoustic frequency, but the minimum -- as well as the maximum -- becomes much higher as the frequency increases. Hence fluctuations caused by waves near mid-range might be undetectable at low frequencies but detectable at high ones.

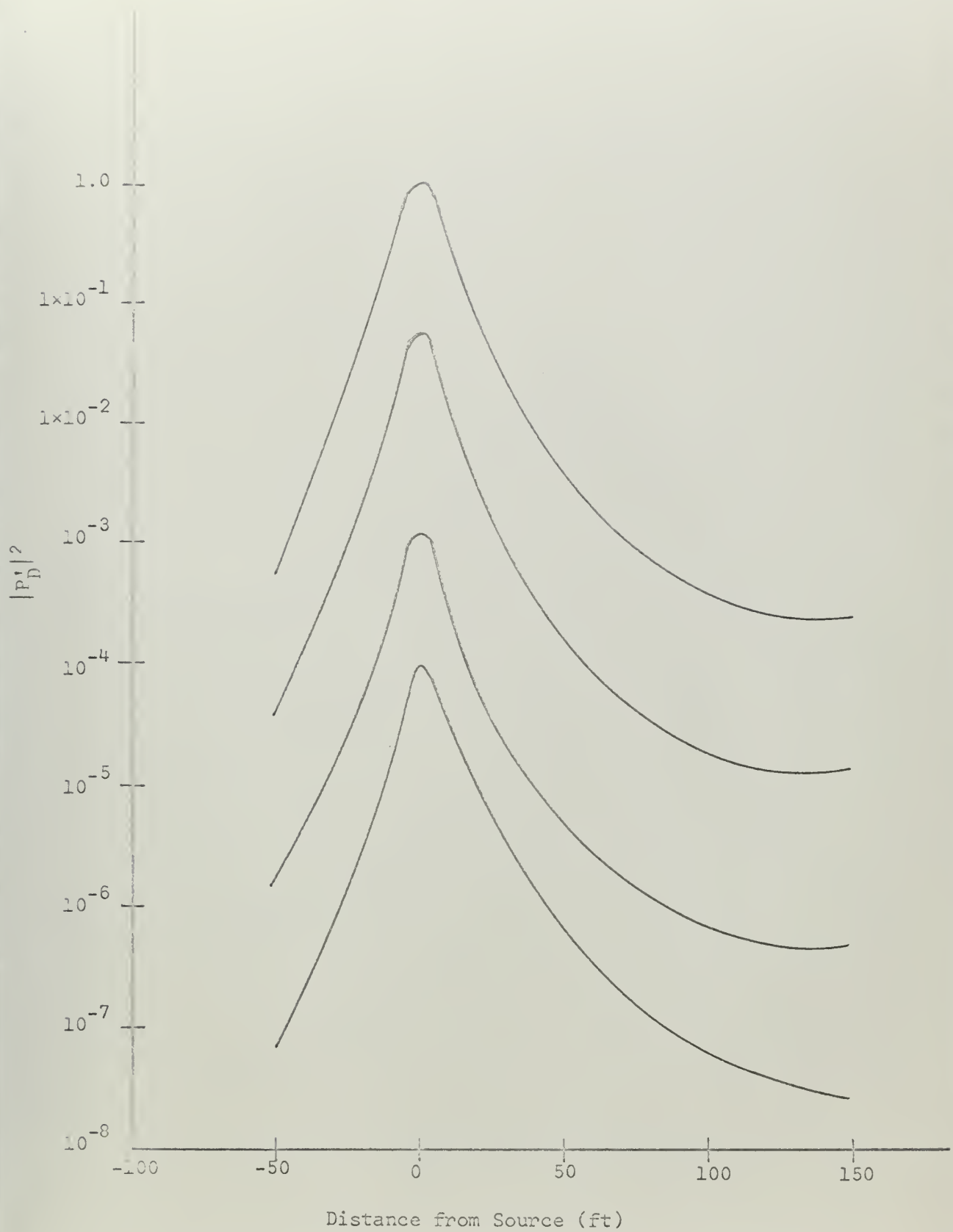


Fig. 7a

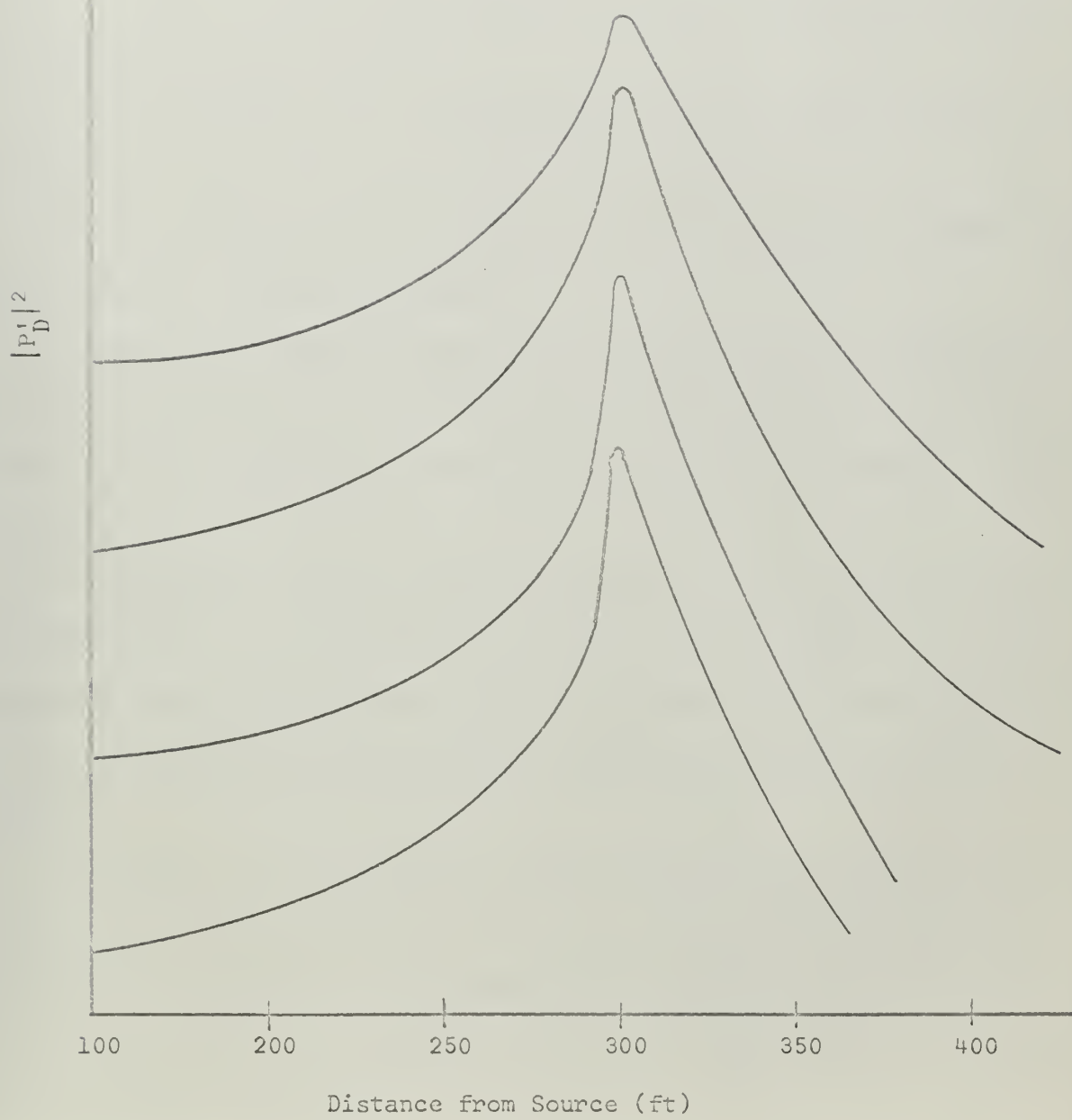


Fig. 7b

In summary our theoretical results are in fair to good agreement with most of Scrimger's measurements, for the lower acoustic frequencies, as outlined below:

1) When the wave pulse is approximately above the source or receiver, $\Delta I/I$ will be far larger than when the pulse is in the mid-range region.

2) At fixed acoustic frequency, $\Delta I/I$ will be proportional to the wave height A .

3) At fixed A , $\Delta I/I$ will rise with frequency at roughly the same rate that Scrimger found (Fig. 4).

4) More generally, $\Delta I/I$ is a function of A/λ , rather than of A or λ separately.

In three other respects, the present theory is not complete enough to be used for comparison with measurements:

5) Agreement in absolute magnitudes of $\Delta I/I$ is not to be expected, until small wave pulses as considered here are joined into trains of several parallel waves extending a considerable distance in the z direction (across the range).

6) Any effects peculiar to high frequencies -- e.g., the saturation shown in Scrimger's Fig. 3, and breakdown of the rule that only waves nearly over the source or receiver are important -- cannot be treated in the present approximation for low frequencies, although Fig. 7 partly corroborates the latter example.

7) Finally, it is not evident why harmonic and other distortions should appear in $\Delta I/I$ (Scrimger's Fig. 9) when A/λ rises above the approximate value $1/18$. Quite possibly our assumption that the wave pulse acts like a simple acoustic dipole fails when the wave height is too great, but this is a surmise and not an explanation.

In an attempt to develop a rudimentary and workable model capable of recreating the experimental conditions, several parameters and boundary conditions were neglected or greatly simplified. These modifications, and suggested refinements of the model, are listed below.

A. Shape of Surface Wave -- In the development of the problem carried out in Section II, and discussed in Section III, the surface-wave perturbation was described as a single symmetric pulse moving from source to receiver. In actual practice, a surface wave, whether natural or produced as the bow-wave disturbance from a boat, is far more complicated. In previous papers published on the subject, surface perturbations have been depicted as being saw-tooth,^{5,6} continuous sinusoid,⁷ and randomly rough,⁸ in shape. In considering the extensive wave patterns described in the Scrimger article, which are formed by wind and by tidal variations, a logical refinement to the single-pulse model presented in this work would be the extension of the concept to produce a continuous wave form (i.e., to represent the disturbed surface as a sinusoidal corrugation).

In the case of Scrimger's bow-wave disturbance, the single-pulse concept can again be extended, this time to produce a wave train of finite length traveling between source and receiver. Since, as noted earlier, the fluctuations are induced mainly by waves near the source and receiver, the question arises as to what portion of this elongated surface wave (the continuous wave or the extended bow-wave) should be considered in determining $\Delta I/I$. A trial-and-error approach

⁵ J. M. Proud, Jr. and P. Tamarkin, J. Appl. Phys. 28, 1298 (1957).

⁶ W. C. Meecham, J. Appl. Phys. 27, 361 (1956).

⁷ E. O. Lacasse, Jr. and P. Tamarkin, J. Appl. Phys. 27, 138 (1956).

⁸ J. M. Proud, Jr., R. T. Beyer and P. Tamarkin, J. Appl. Phys. 31, 543 (1960).

would allow one to find the areas where the surface waves influence the receiver, and to estimate the effect of interference phenomena, but this would prove tedious. No attempt has been made here to solve this additional problem.

The mathematical formulation needed to develop the refinements outlined above follows directly from the initial concepts presented in Section II. Each pulse can be replaced by a dipole, with the relative size of the pulse (i.e., wave height) determining the dipole strength. Thus a decaying wave-form can be represented by a sequence of dipoles of varying strength. In addition, the phase assigned to the point sources making up each dipole can be utilized to distinguish between pulses lying above and below the unperturbed water level. The resulting amplitude recorded at the receiver is then simply the algebraic sum of the contributions due to the individual dipoles, with due regard to phases. A real surface wave does not have equal areas lying above and below the unperturbed surface as indicated in the previous paragraphs. Instead, to an extent depending on the wave height, crests are relatively narrow and high whereas troughs are relatively broad and shallow. Thus, to a first approximation, we could neglect those dipoles lying below the true average surface, allowing our model to consist of a series of "positive" dipoles, lying above a slightly lowered surface, and separated by a finite distance horizontally.

B. Bottom Limitations -- Nowhere in the development of the mathematical model nor subsequently in the results derived from it was mention made of the limitations imposed by the presence of a lower boundary. In considering only the direct ray and the once reflected surface ray (i.e., that ray produced by the perturbation dipole) a substantial simplification is injected into the problem. According to theory, the lower boundary condition usually assumed is that there is a discontinuous "jump" in sound speed across the ocean bottom, from

a lower speed in the water to a higher speed in the sediment. There is also a "jump" in density, in the same sense. The amplitude of the reflected ray will increase from a finite value at normal incidence to a value of unity (i.e., perfect reflection) at a critical angle⁹ and remain unity out to grazing incidence. The phase change is zero from normal incidence out to the critical angle and from there increases in a regular manner to 180 degrees at grazing incidence. It can be demonstrated that the change in amplitude and phase for a reflected plane wave will be given by the Rayleigh reflection coefficients. It can be shown further that this reflection coefficient is valid for spherical waves in the region where the fractional variation in the space rate of change of the amplitude becomes small.¹⁰ In the case under consideration the problem is compounded by the fact that several sediments go into the make-up of the bottom, and the thickness associated with each layer varies along the source-receiver path (see Section I).

As an initial attempt in refining the model to include lower boundary effects, we can consider the bottom to be perfectly level and composed of a single homogeneous material of infinite depth. If we thus assume the bottom to be uniform, as well as "faster" and more dense than the water, the fact that the source and receiver lie well within a wavelength of the bottom presents no problem. If the material beneath the source is considered rigid, it acts like an infinite rigid baffle, and the energy radiated by the source is double that expected in an unbounded medium. By the reciprocity theorem, the receiver now

⁹The critical angle equals $\arcsin(c_1/c_2)$, where c_1 and c_2 are the propagation speed of sound in water and bottom respectively.

¹⁰C. S. Officer, "Introduction to the Theory of Sound Transmission" (McGraw-Hill Book Company, Inc., New York, 1958).

becomes doubly sensitive, so that the overall transmitter-receiver effect increases two-fold. However, since Eq. (3.1) is a ratio of intensities, the increase in the source strength cancels in the expression and does not affect the overall results. The true bottom is not rigid, but it is more dense than the water and possesses a higher sound speed. The qualitative effect will be like that for a rigid bottom, but with factors of less than two.

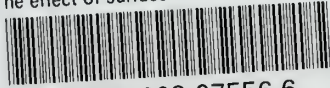
C. Velocity Gradient -- Throughout Sections II and III it was tacitly assumed that an isovelocity gradient existed throughout the shallow water duct. In fact, the Esquimalt Lagoon usually exhibits a slight positive gradient. Under the condition of a positive gradient of sound speed, there is an upward refraction of the rays, and because of this upward bending a larger portion of the energy will be reflected from the bottom at angles of incidence greater than critical. Some rays will be turned upward without undergoing bottom reflection. These characteristics of the positive velocity gradient combine to reduce the loss of energy from the shallow-water duct, thus producing, in general, better transmission characteristics. These effects are, however, important only at long ranges.

The use of 4900 ft/sec as the sound speed in Section III was appropriate since Ref. 1 showed the profile to be isovelocity at this value, from a depth of approximately 3 ft down to the bottom. In general, the procedure in dealing with complicated velocity gradients is to approximate the actual velocity profile as a series of constant slopes, thus allowing for a cumulative solution of each gradient. The partition of the velocity gradient in this case will do little to improve the results, since the source and receiver are bottom-mounted. Thus the downward movement of any ray is quite limited, and for all intents and purposes the velocity profile listed in Ref. 1 can be considered isovelocity.

D. The Dipole Assumption -- Assuming that the acoustic effect of a surface wave pulse can be represented entirely as a simple dipole appears, from the results, to be quite successful. However, for larger wave heights A and shorter acoustic wavelengths λ , this assumption may be an oversimplification. The only portions of experimental evidence pointing this way are the saturation of pressure fluctuations for high values of A/λ , and the harmonic distortion in the spectrum of fluctuations when A/λ exceeds a critical value. Until some other extensions of the theory are completed -- in particular, extensions to wave trains -- there is no conclusive reason for complicating the dipole assumption.

thesH16214

The effect of surface waves on acoustic



3 2768 002 07556 6

DUDLEY KNOX LIBRARY